Article

Efficient Hydroxyapatite Extraction From Salmon Bone Waste: An Improved Lab-Scaled Physico-Chemico-Biological Process

Francisco Muñoz , Ziyad S. Haidar * , Andreu Puigdollers , Ignacio Guerra , Maria Cristina Padilla , Nicole Ortega , Mercedes Balcells , María José García *

Posted Date: 9 July 2024

doi: 10.20944/preprints202311.1090.v2

Keywords: Hydroxyapatite; Salmon Bone; Bone Repair; Biomaterial; Osteoregeneration; Process

Article

Efficient Hydroxyapatite Extraction from Salmon Bone Waste: An Improved Lab-Scaled Physico-Chemico-Biological Process

Francisco Muñoz [1,†], Ziyad S. Haidar [2,3,4,5,6,*,†], A. Puigdollers [7], Ignacio Guerra [1], M. Cristina Padilla [3,4,8,9], Nicole Ortega [8], Mercedes Balcells [10,11] and M. José García [1,*]

1 Facultad de Odontología, Universidad Internacional de Cataluña. Barcelona, Spain
2 Laboratorio BioMAT'X R&D&I (HAiDAR I+D+i LAB), Universidad de los Andes, Santiago, Chile
3 Centro de Investigación e Innovación Biomédica (CiiB), Universidad de los Andes, Santiago, Chile
4 Programa de Doctorado en BioMedicina, Facultad de Medicina, Universidad de los Andes, Santiago, Chile
5 Programa de Doctorado en Ciencias Odontológicas, Facultad de Odontología, Universidad de los Andes, Santiago, Chile
6 Facultad de Odontología, Universidad de los Andes, Santiago, Chile
7 Área de Ortodoncia, Facultat Internacional de Cataluña. Barcelona, Spain
8 Laboratorio de Investigación e Ingeniería de Biopolímeros (BiopREL), Universidad de los Andes, Santiago, Chile
9 Escuela de Nutrición y Dietética, Facultad de Medicina. Universidad de los Andes, Santiago, Chile
10 Institut Quimic de Sarria, Ramon Llull University, Barcelona, Spain
11 MIT Institute for Medical Engineering and Science, Massachusetts Institute of Technology, Cambridge, USA
* Correspondence: zhaidar@uandes.cl (Z.S.H.); mjgarcia12@miuandes.cl (M.J.G.); Tel.: +56996615939 (M.J.G.); Tel.: +56962216694 (Z.S.H.)
† Equal Contribution.

Abstract: Salmon aquaculture generates a substantial volume of waste material, offering potential for biomaterial production. This industry produces significant waste, which can be repurposed for various biological applications, particularly in biomaterial production for tissue engineering with pertinent applications in osteo-conduction, osteo-induction, and clinical/surgical bone regeneration and repair. The process involves a standardized pre-treatment stage aimed at minimizing biological waste content. Subsequently, the treatment stage, contingent on the chosen methodology, facilitates the removal of proteins, lipids, molecules, and other compounds, leaving the mineral phase as a valuable substrate. The selection of the optimal method, whether alkaline hydrolysis, calcination, or NaOH hydrolysis, for obtaining this substrate necessitates thorough examination through chemical, physical, and biological assessments, including Raman Spectroscopy and X-Ray Diffraction. This study aims to identify the most efficient laboratory process for biofunctional nano-sized hydroxyapatite mineral production derived from Chilean salmon fish backbone waste.

Keywords: hydroxyapatite; salmon bone; bone repair; biomaterial; osteoregeneration; process

1. Introduction

In the realm of medicine and dentistry, the quest to address bone defects arising from a myriad of causes, including disease and trauma, stands as a paramount and demanding challenge. Today, this collective endeavor has spurred extensive research into the development of novel biomaterials tailored for bone regeneration, in particular, with a profound impact on our clinical and surgical practice. It is imperative to remember and comprehend that the landscape of bone grafting techniques, given that a diverse array of patients, each presents unique clinical and surgical needs. Thus far, bone grafts can be categorized into four primary groups—autografts, allografts, allografts/alloplastics, and xenografts, each bearing distinct properties tailored to specific indications

 doi:10.20944/preprints202311.1090.v2

and applications; osteoconduction, osteoinduction, osteogenesis and structural support [1]. In fact, the pursuit of effective bone grafting solutions is driven by a substantial demand, with millions (statistically estimated at >2 Million cases in the United States of America, alone) of bone graft procedures performed globally every year [2].

Autografts have long been regarded as the gold standard for bone regeneration due to their superior histocompatibility and all-encompassing characteristics as an ideal bone graft. They offer osteoinduction, osteoconduction, and cellular histocompatibility. However, they are not without their limitations, as they often entail extensive morbidity associated with the donor site, necessitating longer and more expensive hospital admissions than the grafting procedure itself [2]. Allografts, depending on their production methods, serve as osteoconductive biomaterials or even exhibit osteoinductive properties [3]. Their increased availability compared to autografts positions them as viable alternatives; however, they fall short in achieving full regeneration and are scrutinized for potential transmission of viruses and other infectious agents [4]. Some religious beliefs preclude the use of allografts [1]. In contrast, synthetic alloplastic materials, while lacking osteogenic and osteoinductive potential, excel in promoting osteoconduction by serving as a scaffold for bone regeneration. The level of porosity, reabsorption capacity, and crystallinity, pivotal features of biomaterials, hinges predominantly on the manufacturing process [1,5]. Lastly, xenografts, devoid of osteogenic potential, face varying levels of acceptance depending on the species they originate (or, are sourced) from, with some faiths/religions, traditions, customs and cultures opposing their use [6]. Despite these limitations and drawbacks, scaffold osteoconduction remains effective and widely available, circumventing the complications associated with allografts and autografts [2].

In the domain of bioceramic materials, diversity reigns, contingent upon the specific species of origin from which they are sourced. To uncover the optimal characteristics while simultaneously streamlining production costs, relentless efforts have been invested in the production and creation of osteoconductive and osteoinductive biomaterials derived from various species, including but not limited to bovine, porcine, mollusks, and fish [5]. Within this perpetual quest, a notable breakthrough has recently emerged—namely, the isolation, extraction, and production of hydroxyapatite (HA) from the bones of salmon fish (waste), offering a two-fold advantage: sustainability and biocompatibility. Indeed, the salmon industry predominantly focuses on the commercialization of salmon fillets, resulting in a surplus of byproducts, encompassing heads, entrails, scales, and bones, which are often disproportionately discarded into the environment, causing ecological (eco-system) harm/damage [7–9]. This surplus of waste represents a novel opportunity for sustainable waste management and re-purposing. Notably, R&D&I (research, development and innovation) findings have thus far indicated that this HA bioceramic material demonstrates impressive biocompatibility, as evidenced by *in vitro* tests revealing an absence of cytotoxicity [9]. Moreover, Shi *et al*. underscored an additional advantage, wherein salmon-derived HA is enriched with vital mineral ions that foster enhanced cell proliferation, differentiation, adhesion, and the formation of mineralized tissue. This stark contrast to bioceramics obtained from other fish species, such as tuna or cod, suggests an innovative edge to salmon-based bioceramics [9]. In addition, Venkatesan *et al*. emphasized that the significant evolutionary gap between humans and fish considerably diminishes the risk of disease transmission, thus further augmenting the appeal of salmon-derived bioceramics [8–12]. Henceforth, in essence, R&D&I has showcased the multi-faceted potential of salmon fish backbone HA, heralding a new era of sustainable molecules and biomaterials that also align with stringent biocompatibility standards, marking a significant stride in the field of regenerative medicine and dentistry; an ongoing *hot* topic in our collaborative laboratories. Indeed, we have recently reported the physico-chemical properties of our *patent-pending* nano-scaled HA material obtained from the backbone of salmon fish [10]. Briefly, our nanoS-HAp is obtained via a modified and innovative alkaline hydrolysis-calcination process, followed by characterization using by X-ray diffraction, electron microscopy, spectroscopy, and cell viability assays. When compared to control HAp (synthetic, human, bovine or porcine), our nanoS-HAp demonstrated attractive characteristics, rendering it a promising biomaterial candidate for use in simple/complex bone tissue engineering indications, and beyond [10].

 doi:10.20944/preprints202311.1090.v2

The primary aim of the present study is to investigate mechanisms for the efficient and cost-effective isolation and extraction of hydroxyapatite from salmon fish bones, yielding workable biomaterials with osteoinductive potential. This would also contribute to a more sustainable utilization of waste generated by the salmon industry, a prominent Chilean resource. Henceforth, salmon fish bones consist of two primary phases: organic and mineral. The mineral phase is isolated during the HA extraction process. Herein, we conducted distinctive protocols within our laboratory, drawn from relevant literature [9,12–14], for comparative purposes. These were carefully replicated and subjected to lab-scaled characterization via Raman Spectrometry followed by X-Ray Diffraction to ensure both reproducibility and to gain initial insights into the physical attributes of the resultant material; thereby reporting our *patent-pending* nanoS-Hap prep protocol.

2. Material and Methods

The HA extraction and production process involved, primarily, an extensive literature review of articles between the period of 2015 to 2020, wherein the bioceramic extraction process from salmon fish bone (of any type) was described. Henceforth, three published studies [9,12,13] were finally selected to assess the described protocols and if could be replicated in various facilities at the CiiB of Universidad de los Andes, Santiago de Chile. Modification, customization and calibration of the final prep protocol followed.

A preliminary bone pre-treatment protocol was executed, initiated by submerging the bone in purified water obtained through reverse osmosis (H_2Op; p for purified) and maintaining it *heated* at a temperature of 35°C for a duration of 12 hours (hrs). Subsequently, the removal process entailed manually extracting the spines and larger voluminous muscle pieces. The vertebrae were then segregated/separated and preserved in storage within the temperature range of -18°C to -25°C. This protocol encompassed six sequential steps. Following an adapted and a modified version of Shi *et al.*'s protocol (Figure 1), the salmon fish bone underwent separation, thawing, and weighing. A 1:2 weight-to-volume ratio (bone weight to water volume; w/v) of H_2Op was heated to 95°C and stirred at 200 revolutions per minute (rpm) using a magnetic stirrer (Dlab; MS-H-Pro+; China). Once the desired temperature was attained, the bone was then introduced/added, and the specified temperature and stirring conditions were consistently maintained for 1 hr. Subsequently, the liquid was separated by drainage using a fine metal strainer (Ilko®; 10cm Inox). A rinsing/washing step/process was carried out three times in a standard magnetic stirrer with H_2Op, maintaining the 1:2 w/v ratio, while continuously/constantly agitating at 150 rpm for 5 minutes, each time. Following the drainage and removal of the liquid using the strainer, a 1 Molar (M) solution of Merck® sodium hydroxide (NaOH) was added at the standard 1:2 w/v ratio and left to react for 24 hrs, with constant stirring at 200 rpm. Afterwards, the liquid was once again separated using the described strainer, and the resultant material was subjected to three incessant washing cycles inside the magnetic stirrer with H_2Op, maintaining a 1:1 w/v ratio and agitating it at 200 rpm for 5 minutes in each cycle. The bone was subsequently immersed/submerged in acetone (Sigma-Aldrich) at a 1:1 w/v ratio and placed on the magnetic stirrer operating at 200 rpm for 24 hrs. The solution was then decanted with the aid of the strainer and underwent three sequential washing cycles with H_2Op, preserving the 1:1 w/v ratio, on a magnetic stirrer rotating at 250 rpm for 5 minutes, for each cycle. The resulting material was then subjected to a drying process in an oven (Horizontal flow; WOF-105; China) set at 60°C for a period of 12 hrs. The crucibles used in the process were also dried in the oven set at 60°C for 30 minutes. Upon reaching/achieving a dry and moisture-free state, the crucibles were weighed and measured using a Shimadzu (AUX 120; China) analytical balance. Subsequently, the grinding procedure was carried out using a rotor mill (Foss; KN 295 Knifetec; China), consisting of four pulses, each lasting 2 seconds. Following this, the electric Muffle Furnace (XL-1000c/1200c/1600c; China) was pre-heated to 650°C. Once the desired temperature was attained, the sample was subjected to calcination for 5 hrs, after which it was allowed to cool within the Muffle Furnace for an additional 60 minutes. Finally, the resultant final material and sample(s) was/were weighed, labeled, and properly stored in an environment devoid of moisture, maintained at -80°C and shielded from any exposure to light. It is noteworthy herein that to ensure the reproducibility of the HA extraction

 doi:10.20944/preprints202311.1090.v2

procedure, the designed and performed protocol was duplicated on two separate occasions, under the same conditions. The samples were subsequently subjected to Raman Spectrometry. This protocol was once again replicated then underwent a comprehensive characterization through both, Raman Spectrometry and X-Ray Diffraction, following the pre-established methodologies [9–13,15] and introduced/applied standardizations at our R&D&I laboratories.

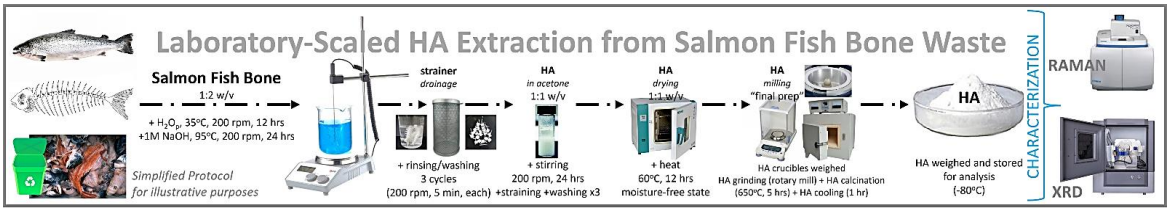

Figure 1. Illustrating the Prep Protocol for Hydroxyapatite Extraction from Salmon Bone Waste.

3. Results

3.1. Characterization

In the present study, two essential characterization tests, namely Raman Spectrometry and X-Ray powder Diffraction, were employed to assess the obtained salmon fish bone bio-ceramic. The Raman scattering spectroscopy measurements of the HA obtained by mechanical alloying were obtained. Briefly, the Raman spectra were measured using a triple monochromator micro-Raman spectrometer, equipped with a charged coupled device (CCD) detector, and using the 4880 Å exciting line of the Ar-laser. XRD was also performed using an X-ray diffractometer (Phillips X'Pert Pro, UK) equipped with a CuKα radiation source set at 1,541 Å wavelength, to analyze the anatomical and molecular structure of the obtained HA crystals. Studies were run at a current of 30 mA and an accelerating voltage of 40 Kv, over the 2θ diffraction angle range of 2° to 80° using a step size of 0.02°. The patterns obtained were analyzed using the Origin pro 2019b software (OriginLab Corp., USA). Further, scanning electron microscopy (SEM) and energy dispersive X-ray spectroscopy (EDS) were used to evaluate the Ca/P ratio within samples (Figure 2). Briefly, a Carl Zeiss scanning electron microscope (EVO MA 10, Oberkochen, Germany) equipped with energy dispersive spectroscopy was used to analyze the chemical composition of the samples. All these analyses were done at our labs within the CiiB.

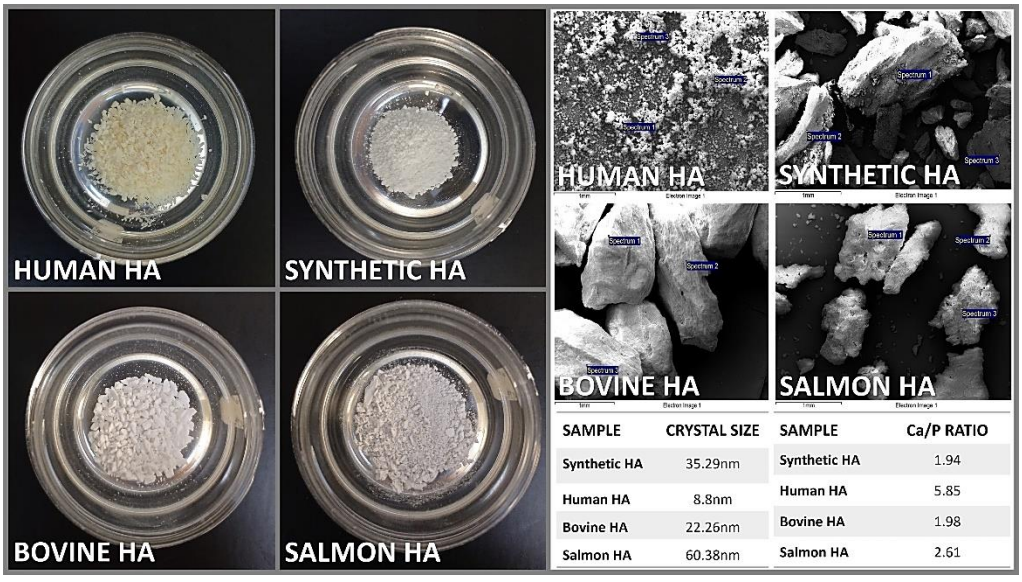

Figure 2. Prepared control and experimental HA samples (*LEFT*) before characterization and analysis. SEM micrographs of control and experimental HA samples (*TOP RIGHT*). Crystal size control and experimental HA samples obtained by XRD and Ca/P ratio (atomic weight %) for control and experimental HA samples obtained by SEM/EDS (*BOTTOM RIGHT*). The crystal size studied using

 doi:10.20944/preprints202311.1090.v2

XRD and further analyzed using the Scherrer equation, reported sizes ranging from 8.8 nm to 60.38 nm. Using SEM/EDS analysis, the Ca/P ratio (atomic weight %)* for the samples determined the lowest values for our salmon HA and bovine HA with 1.94 and 1.98 respectively, yet similar/close to what is often presented in the literature (*stoichiometric value of HA set at 1.67*), validating our experimental protocol. It is noteworthy that all other HA yielded values higher than commonly reported in the literature. * The Ca/P ratio (calcium to phosphorus ratio) in terms of atomic weight percentage (%) is calculated by dividing the atomic weight % of calcium (Ca) by the atomic weight % of phosphorus (P). The atomic weights of Ca and P, approximately are 40.08 g/mol and 30.97 g/mol, respectively. As aforementioned, human HA, has a Ca/P ratio close to 1.67 in ideal form. Deviations from this ratio can indicate changes in bone mineral density and quality.

The initial phase of the analysis involved Raman Spectrometry (Raman 1), aimed at evaluating the replicability of the material and confirming the presence of hydroxyapatite functional groups (Figure 3). A commercially-available synthetic HA sample obtained from Sigma-Aldrich served as a reference control, for comparison. This test provided an initial insight into the characteristics of the obtained material while validating the existence of HA functional groups in the control. To ensure the consistency and reliability of the obtained data and findings, the experimental protocol was accurately duplicated, and the resulting sample underwent a secondary round of Raman Spectrometry analysis (Raman 2). Additionally, X-ray Diffraction (XRD 1) was carried out, using the synthetic HA sample from Sigma-Aldrich as a control for reference (Figure 4). These characterization tests, to the best of our knowledge, collectively, provided a comprehensive evaluation of the composition and properties of this salmon fish bone bio-ceramic.

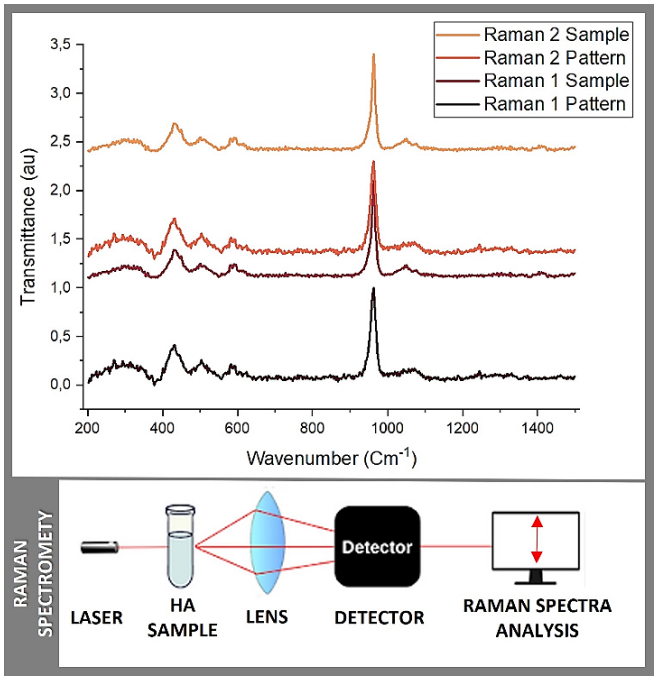

Figure 3. Raman spectrometry: Raman 1 and Raman 2 measurements.

Preprints.org (www.preprints.org) | NOT PEER-REVIEWED | Posted: 9 July 2024 doi:10.20944/preprints202311.1090.v2

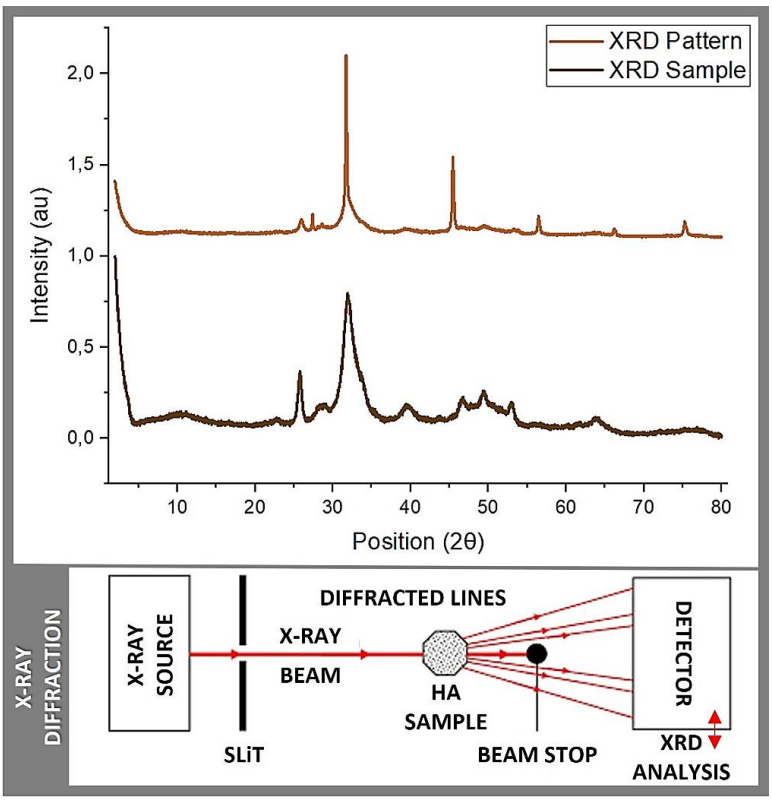

Figure 4. XRD: XRD pattern and sample measurements.

3.2. Raman Spectrometry

Raman Spectrometry is a versatile technique used for the analysis of molecular vibrations in a wide range of materials, from solids to liquids and gases. It is a non-invasive and non-destructive method widely used in research, industry, and various scientific disciplines. It provides valuable information about chemical composition, molecular structure, and crystal symmetry. Briefly, each chemical bond in a molecule vibrates at specific frequencies, and these vibrations are detected in the Raman spectrum, allowing for chemical identification. Hence, Raman spectroscopy provides insights into the molecular structure and symmetry of a material via revealing details about bond lengths, angles, and the arrangement of atoms within molecules. Further, it can distinguish between different phases of a material, including polymorphs, crystal structures, and amorphous phases. It is useful for materials science and crystallography. Raman spectrometry can also be used to investigate the stress and strain in a material where changes in vibrational frequencies can indicate mechanical stresses within the sample. Last yet not least, it is often employed for quality control assessment and process monitoring in various industries, including pharmaceuticals, food, and bio-materials sciences.

Raman spectrometry was principally used in this study to identify the functional groups in the prepared sample(s) in order to establish an approximation of the HA structure and to confirm the calcium phosphates (CaP) basic structure units. The results obtained from Raman 1 and Raman 2 are reported in Table 1 and Figure 3. Briefly, hydroxide (OH), phosphate ion (PO_4) and carbon trioxide (CO_3) were present in both batches of samples, as in most CaP. In addition, different bands such as 623 cm^{-1}, 759 cm^{-1}, 819 cm^{-1}, 845 cm^{-1}, and 882 cm^{-1} corresponding to the reference spectra reported in the literature were detected/measured [16]. These ranges showed exact coincidences and other significant peaks. The first zone of exact coincidence showed common peak ranges, oscillating between 580 cm^{-1} and 589 cm^{-1}, with an average of 580 cm^{-1}. Such range (*i.e.* 580 cm^{-1})corresponds to a symmetric P-O stretching vibration (*simultaneous vibration of two bonds, in which the bonds elongate together and contract together*) n4 [16], typical of the functional group PO_4, and characteristic of tetrahedral *biological* apatites [15], often reported in the literature [15,17]. A second zone of exact coincidence corresponds to a 961 cm^{-1} peak, with the highest spectrum intensity, described as the PO_4 groups bending mode and PO_4 vibrations [18]. Associated with this same functional group, a lower

 doi:10.20944/preprints202311.1090.v2

intensity peak formed around 1070 cm^{-1} - 1074 cm^{-1} is described as PO_4 bands stretching vibration [18]. Additionally, some peaks are present only in a few samples. The obtained peaks of 595 cm^{-1} (Raman1) and 623 cm^{-1} (Raman 2) correlate with 602 cm^{-1} - 603 cm^{-1} or 632 cm^{-1} - 635 cm^{-1} belonging to the OH groups [15]. Stretching and liberation modes of OH are typical of HA crystallites structures [15]. Finally, a 1460 cm^{-1} peak is reported in Raman 2, which could be related to the presence of a CO_3 group. Research shows that this peak can occur between 1421 cm^{-1} and 1466 cm^{-1}. Its presence in bone graft materials is described as a factor that allows to simulate the extracellular matrix (ECM), the intricate network of proteins and minerals found in native bone tissue, which in turn would improve osseointegration, biocompatibility and *earl* osseous resorption [19]. Herein, similar to porosity, a critically important factor that allows for the simulation of the ECM whereby introducing controlled porosity in bone graft materials, it becomes possible to replicate the natural structure of the ECM via serving as a scaffold that promotes cell attachment, proliferation, and differentiation whilst allowing for the ingrowth of blood vessels and the formation of new or *de novo* bone tissue. Indeed, the presence of this ECM-like porosity in bone graft materials enhances osseointegration and the bone tissue regenerative outcome, as it provides a mechanically-supportive and biomimetic environment suitable for the interaction (effective fusion) between the host cells, native bone, and the graft material. It also improves biocompatibility through mimicking the natural bone micro-environment (more conducive to cell adhesion, proliferation, and differentiation, closely resembling the natural bone micro-environment of the patient). In addition, controlled porosity can lead to *early* bone resorption, as mentioned above, a desirable feature in bone graft materials, as it allows the material to gradually bio-degrade and be substituted by the own bone tissue of the patient during the healing process [19,20].

Table 1. Sample description and functional group interpretation according to the KnowItAll® HORIBA Edition software and Raman database that includes over 1500 spectra for comparative analysis, SearchIt™ for database spectral searching, MineIt™ for database visualization and mining and Mixture Analysis which identifies individual component(s) in a mixture spectrum, through a database searching.

Raman 1 Pattern	Raman 1 Sample	Raman 2 Pattern	Raman 2 Sample	HORIBA Scientific Raman Database*
307,572	-	307,572	-	δ(CC) aliphatic chains
-	269,532	-	269,532	δ(CC) aliphatic chains
-	292,969	-	292,969	υ(Se-Se)
-	313,404	-	313,404	υ(Se-Se)
428,881	-	428,881	-	υ(S-S)
-	431,74	-	431,74	υ(S-S)
448,8075	-	448,8075	-	υ(Si-O-Si)
499,951	-	499,951	-	υ(Si-O-Si)
-	502,777	-	502,77	υ(Si-O-Si)
580,40886	581,35	589,707	581,35	υ(C-Cl)
614,708	-	-	623,019	υ(C-I)
727,278	-	-	759,819	υ(C-S) aliphatic
961,748	961,748	961,748	961,748	ν 1 (PO4 3−) /(A/E2)
1049,81	-	1049,81	-	υ(C=S)
1074,87223	1071,03918	1074,87223	1070,33	υ(C=S)
-	1244,80409	-	1244,23	υ(C=S)

**KnowItAll® Informatics System; a spectra database covering many applications, available for data mining, analytical and comparative studies, from HORIBA Scientific, Japan.*

3.3. X-ray Diffraction

The main objective of X-ray diffraction (XRD) is to determine the atomic and molecular structure (phase) of a crystalline material. XRD helps in identifying hydroxyapatite and distinguishing it from

 doi:10.20944/preprints202311.1090.v2

other calcium phosphate phases such as tricalcium phosphate and dicalcium phosphate, where each phase has a unique diffraction pattern. In this context, XRD is a powerful characterization tool, widely used analytical technique in materials science, chemistry, and related fields. It involves shining X-rays onto a crystalline sample and observing the resulting diffraction pattern, which is caused by the interference of X-rays scattered by the crystal lattice. Indeed, XRD can determine the crystal composition and structure of a material, which describes the arrangement of atoms or molecules within the crystal lattice. It reveals the unit cell dimensions, atomic positions, and symmetry of the crystal. Moreover, XRD is used to identify the different phases present in a sample, which is crucial for materials characterization. It can differentiate between various polymorphs or crystal structures of the same material. Further, XRD can quantify the degree of crystallinity (degree of crystallinity is a measure of the fraction of a material that is crystalline compared to the amorphous or non-crystalline phase. It significantly influences the physical properties of the material, such as mechanical strength, thermal stability, and chemical resistance; *i.e.* higher crystallinity usually indicates better stability and mechanical strength.) in a sample, providing information about the order or disorder of the crystal lattice. XRD also measures the lattice parameters, which include the lengths of the edges of the unit cell (a, b, and c) and the angles between them (α, β, and γ). These parameters are fundamental in defining the crystal structure and can provide significant insights into the properties and behavior of the material/biomaterial. Henceforth, XRD can be used to assess the stress and strain within a crystal lattice, which is important in materials engineering and quality control. Last yet not least, XRD is vital in providing critical information about the size and distribution of crystalline particles in a biomaterial.

In this context, Table 2, and Figure 4 display the results obtained from the conducted quantitative analysis, in which the following spectra were compared: the sample obtained in this study, a JCPDS 74-0565 (*standards compiled by the Joint Committee on Powder Diffraction Standards*) pattern, the sample reported by Shi *et al*. based on salmon fish bone and the control sample corresponding to commercially available HA (Sigma-Aldrich). In relation to the data obtained, 5 bands of transversal coincidence were found for the 4 spectra, all in the range between 20 and 60 2Theta, which belong to the characteristic peaks of CaP (calcium phosphates) that are located 25, 31, 39, 46, 49 and 53 2Theta.

Table 2. XRD spectra of bio-ceramics obtained from salmon fish bone compared with the spectra of synthetic HA (Sigma-Aldrich) and the spectras reported in JCPDS 74-0565 and Shi *et al*, respectively.

JCPDS 74-0565*	Shi *et al.* Natural HA	HA Sigma Aldrich	Salmon Fish Bone Bio-Ceramic
-	-	10,8	10,43
25,882	25,845	25,81	25,9
-	-	28,08	28,37
-	-	28,89	28,5
-	-	29,64	29,16
31,765	31,792	31,73	31,6
32,194	32,142	32,13	-
32,896	32,935	32,86	-
34,062	34,055	34	-
39,79	39,816	39,74	39,46
-	-	45,25	45,41
46,693	46,698	46,61	46,72
-	-	48,01	48,04
49,489	49,496	49,39	49,42
50,474	50,568	50,42	-
-	-	51,21	51,41
53,218	53,183	53,1	53,27
-	-	57,8	56,43

 doi:10.20944/preprints202311.1090.v2

-	-	62,93	63,84
-	-	66,26	66,17
-	-	75,49	75,25

** JCPDS 74-0565: Joint Committee on Powder Diffraction Standards*

The obtained spectra have the characteristic defined and sharp shape, proper of crystalline structures. In addition, when contrasting the samples against the Crystallography Open Database (COD) and COD inorganic compounds only (CODI), using the Match 3! Software; *an easy-to-use software for phase analysis using powder diffraction data and compares the diffraction pattern of your sample to a database*, the presence of Ca, P and O in different structural combinations was confirmed. The analyzed samples correspond to the essential sub-units of CaP, yet more studies are required to better define their arrangement and the Ca:P ratio. Along with this, traces of elements such as Sr and/or Mg were found, potentially beneficial for the biocompatibility of bone graft materials [19,20]. Regarding the conducted qualitative analysis of the samples obtained, the crystal size was measured using the Scherrer equation, which resulted in an average crystal size of 130.1 Å for the bio-ceramics obtained from the salmon fish bone. For the HA control sample (Sigma-Aldrich), an average value of crystal size of 285.8 Å was obtained. Both crystal sizes when transformed into nm, corresponded to 13.01 and 25.58 nm, respectively, which are close to the values reported in literature for this type of material [12–15] (*please re-visit data in* Table 2).

4. Discussion

4.1. Production

Today, the realm of bone regeneration material production has seen substantial R&D&I efforts, with a drive towards developing cost-effective and readily available alternatives to address the challenges of high production costs and storage, amongst others. This pursuit has led to the exploration of novel sources for xenograft-type materials, which have the potential to reduce expenses, enhance biocompatibility, improve cellular and biological interactions, and increase availability. In this context, xenografts derived from fish bones have captured the interest of R&D&I groups and laboratories, including ours.

Various methods for producing these xenografts, such as NaOH-based hydrolysis, calcination, and enzymatic hydrolysis, have been reported in the accruing literature. The aim of our present study was to study and describe the process for extracting the mineral phase from salmon fish bones, for the development of a new reproducible protocol based largely on the framework previously proposed by Shi *et al*. [9], deemed most suitable and practical. Indeed, this protocol focuses on *key* elements, factors and stages designed to eliminate a significant portion of organic matter. Such involved the thorough cleaning and removal/elimination of large-scale muscle tissue at elevated temperatures, enzymatic lysis of collagen and proteins in the bone matrix using an appropriate concentration of NaOH, removal of lipids and fats through de-fatting in an acetone solution, and finally, the calcination process to eliminate residual (from previous processes/stages) organic components. Herein, it is crucial to exercise extreme caution to avoid/prevent any damage to the bone mineral matrix, as any remaining residues could potentially alter the structural integrity or act as a vector for contamination [9–15]. As presented in our study, we proposed, designed and developed an innovative and patent-pending experimental preparation protocol for extracting and producing HA and nano-scaled HA bio-ceramic material from salmon fish bones, which co-integrates alkaline hydrolysis, de-fatting, and calcination processes. This simplified and reproducible approach offers a simple, efficient, and inexpensive method for advancing the extraction, formulation and production of bone regeneration biomaterials from sustainable and readily available resource(s), possibly impacting the field of functional biomaterials.

4.2. Characterization

 doi:10.20944/preprints202311.1090.v2

To obtain a preliminary insight into the structure of the extracted material, we conducted Raman spectrometry and XRD analyses. Following the initial/primary characterization, we verified the reproducibility of our results, observing a high degree of consistency and satisfactory coherence across the different sample batches. In our Raman spectrometry results, we confirmed the presence of the essential functional groups crucial for the formation of HA or beta-tricalcium phosphate (ß-TCP), such as PO_4, OH, and CaO_3. Notably, the characteristic peaks corresponding to these functional groups were consistently detected in all compared samples. To ensure precision and confirm the presence of HA, we performed two sets of comparisons with the selected controls, revealing a very close match. This was particularly evident in the peak with the highest volume, associated with one of the PO_4 functional group bands. Additionally, the presence of a CO_3^{-2} group, reported in the 1421 cm^{-1} - 1466 cm^{-1} peak range (in the Raman 2 set), is linked, in the literature, to enhanced biocompatibility in bone regeneration materials. As a point of reference, herein, we employed synthetic and commercially-available HA (Sigma-Aldrich) as a control [15–20]. The XRD analysis confirmed the presence of key elements like Ca, P, and O, as well as trace elements including Sr and Mg. These trace elements have been identified as potential contributors to the biocompatibility of the regenerative material, consistent with previous research and literature. It is perhaps noteworthy that although we did not find an exact match in the databases (COD and CODI) used, our findings do align with the expected distribution of a crystalline structure and an estimated crystal size, as described in the literature and suitable for osseo-regenerative and -reparative materials of this type [19,20]. Collectively, these results support the further exploration and use of salmon-derived materials for tissue (hard and potentially, soft) repair and regeneration, hereby, indicating their potential advantages over alternatives derived from other fish species, and highlighting their practical promise as a valuable resource for the development of new tissue engineering biomaterial(s).

To summarize, based on the results obtained during this characterization, a microscopic and structural resemblance can be established with other bio-ceramic materials derived from salmon fish bone, as reported in the existing literature. These materials are primarily composed of HA, ß-TCP, or a combination of both. However, to gain a comprehensive understanding of the properties, additional physical characterization tests should be conducted on our produced material. For example, besides the conducted SEM recommended to define the surface topography, surface morphology, pore size, and its Ca/P ratio, other microscopy techniques can be also employed. Furthermore, conducting compression tests would provide insights into its compressive strength and compaction potential [9,15,18–20]. In terms of chemical analysis, thermo-gravimetric analysis can help assess the purity of the sample via quantifying the organic content and moisture. This analysis will be valuable in determining the composition of the final material [9,14,15,18–20]. To evaluate its suitability for biological applications, it is essential to conduct biological tests designed for assessing cyto-/bio-compatibility and efficacy. These tests may include analyses of cell proliferation and alkaline phosphatase activity to determine the ability of the material to support cell proliferation and differentiation, respectively. Such experiments are ongoing in our labs, including pre-clinical *in vivo* assays in suitable models. Until these thorough assessments are performed, we cannot provide an exact composition or behaviour prediction of the material upon clinical/surgical use. However, the lab-scale material we have obtained, under controlled conditions, presents itself as a promising candidate for use in bone tissue repair and regeneration. Its similarities to the various employed control materials as well as other reported materials in the literature suggest its potential for such compound application(s).

5. Conclusions

The isolated functional biomaterial from salmon fish bone demonstrates favorable bio-chemical properties denoted by the presence of bioactive HA containing mineral ions, for instance, positioning it as a viable candidate to produce (lab-scaled, to date) xenografts suitable for bone repair and regeneration applications. The straightforward/simplified, reproducible and inexpensive extraction and production process, method and/or protocol is not only environmentally sustainable yet also

 doi:10.20944/preprints202311.1090.v2

addresses the challenging issue of *isolating* bio-waste generated by the salmon sector, in particular, and the wider marine and aquatic industry, in general. Nonetheless, it is imperative to underscore that further in-depth characterization is essential to fully realize the capabilities and suitability of this natural bio-ceramic material for diverse bio-medical and -dental applications in the field of bone regeneration; a continuing R&D&I endeavor in our labs.

Author Contributions: Conceptualization, F.M. and Z.S.H.; Methodology, F.M., A.P. and Z.S.H.; Investigation, I.G., M.C.P., M.J.G., N.O. and Z.S.H., Writing—original draft preparation, F.M., M.B., M.J.G. and Z.S.H.; Writing—review and editing, Z.S.H; Final version review/editing: Z.S.H. All authors have read and agreed to this manuscript.

Funding: This research work was supported by operating grants provided to the HAiDAR R&D&I LAB/BioMAT'X (Laboratorio de Biomateriales, Farmacéuticos y Bioingeniería de Tejidos Cráneo Máxilo-Facial), member of CiiB (Centro de Investigación e Innovación Biomédica), Faculties of Medicine and Dentistry, Universidad de los Andes, Santiago de Chile, through the ANID-NAM (Agencia Nacional de Investigación y Desarrollo, Chile and National Academy of Medicine, USA) Grant código # **NAM21I0022 (2020-2022)**, CORFO Crea y Valida I+D+i Grant código # **21CVC2-183649 (2021-2023)**, CORFO Crea y Valida — Proyecto de I+D+i Colaborativo - Reactívate" Grant código # **22CVC2-218196 (2022-2024)**, and FONDEF Concurso IDeA de I+D, ANID, Grant código # **ID22I10215 (2022-2024)**. Finally, the authors are pleased to particularly acknowledge the awarded CORFO Crea y Valida I+D+i Grant dedicated to Salmon Fish Bone Código # **21CVC2-183641 (2022-2024)**.

Data Availability Statement: All raw data underlying the results are included herein and no additional source data is required.

Acknowledgments: The authors wish to acknowledge the contributions of veterinarian Ms. Nataly Quezada, member of our CiiB team, for her invaluable support to this work.

Conflicts of Interest: The authors declare that the research was conducted in the absence of any commercial or financial relationships that could be construed as a potential conflict of interest.

Patents: Patent Cooperation Treaty (PCT) – (International) has been filed by the co-authors of this article.

References

1. Fillingham, Y.; Jacobs, J. Bone grafts and their substitutes. *Bone Joint J* **2016**, *98-B*(1 Suppl A). 6-9.
2. Fillingham, Y.A.; Lenart, B.A.; Gitelis, S. Function after injection of benign bone lesions with a bioceramic. *Clin Orthop Relat Res* **2012**, *470*(7); 2014-20.
3. Finkemeier, C.G. Bone-grafting and bone-graft substitutes. *J Bone Joint Surg Am* **2002**, *84*(3), 454-64.
4. De Long, W.G.; Einhorn, T.A.; Koval, K.; McKee, M.; Smith, W.; Sanders, R., *et al*. Bone grafts and bone graft substitutes in orthopaedic trauma surgery. A critical analysis. *J Bone Joint Surg Am* **2007**, *89*(3), 649-58.
5. Salgado, A.J.; Coutinho, O.P.; Reis, R.L. Bone tissue engineering: state of the art and future trends. *Macromol Biosci* **2004**, *4*(8), 743-65.
6. Gómez-Guillén, M.C.; Giménez, B.; López-Caballero, M.E.; Montero, M.P. Functional and bioactive properties of collagen and gelatin from alternative sources: A review. *Food Hydrocolloids* **2011**, *25*(8), 1813-27.
7. Malde, M.K.; Graff, I.E.; Siljander-Rasi, H.; Venäläinen, E.; Julshamn, K.; Pedersen, J.I.; Valaja, J. ORIGINAL ARTICLE: fish bones – a highly available calcium source for growing pigs. *J Anim Physiol Anim Nutr* **2010**, 94:e66–76. doi: 10.1111/j.1439-0396.2009.00979.x
8. Venkatesan, J.; Ryu, B.; Sudha, P.N.; Kim, S-K. Preparation and characterization of chitosan-carbon nanotube scaffolds for bone tissue engineering. *Int J Biol Macromol* **2012**, *50*(2), 393-402.
9. Shi, P.; Liu, M.; Fan, F.; Yu, C.; Lu, W.; Du, M. Characterization of natural hydroxyapatite originated from fish bone and its biocompatibility with osteoblasts. *Mater Sci Eng C Mater Biol Appl* **2018**, *90*, 706-12.
10. Muñoz, F.; Haidar, Z.S.; Puigdollers, A.; Guerra, I.; Padilla, M.C.; Ortega, N.; García, M.J. A novel Chilean salmon fish backbone-based nanoHydroxyApatite functional biomaterial for potential use in bone tissue engineering. *Frontiers in Medicine*, **2024**; 11:1330482. doi: 10.3389/fmed.2024.1330482.
11. Hoyer, B.; Bernhardt, A.; Heinemann, S.; Stachel, I.; Meyer, M.; Gelinsky, M. Biomimetically mineralized salmon collagen scaffolds for application in bone tissue engineering. *Biomacromolecules* **2012**, *13*(4), 1059-66.
12. Venkatesan, J.; Lowe, B.; Manivasagan, P.; Kang, K-H; Chalisserry, E.P.; Anil, S.; *et al*. Isolation and Characterization of Nano-Hydroxyapatite from Salmon Fish Bone. *Materials* (Basel), **2015**, *8*(8), 5426-39.
13. Idowu, A.T.; Benjakul, S.; Sinthusamran, S.; Sae-leaw, T.; Suzuki, N.; Kitani, Y.; *et al*. Effect of Alkaline Treatment on Characteristics of Bio-Calcium and Hydroxyapatite Powders Derived from Salmon Bone. *Applied Sciences* **2020**, *10*(4141), 4141.

 doi:10.20944/preprints202311.1090.v2

14. Kotak, D.J.; Devarajan, P.V. Bone targeted delivery of salmon calcitonin hydroxyapatite nanoparticles for sublingual osteoporosis therapy (SLOT). *Nanomedicine* **2020**, *24*, 102153.
15. Bas, M.; Daglilar, S.; Kuskonmaz, N.; Kalkandelen, C.; Erdemir, G.; Kuruca, S.E.; *et al*. Mechanical and Biocompatibility Properties of Calcium Phosphate Bioceramics Derived from Salmon Fish Bone Wastes. *Int J Mol Sci* **2020**, *21*(21).
16. Koutsopoulos, S. Synthesis and characterization of hydroxyapatite crystals: a review study on the analytical methods. *J Biomed Mater Res* **2002**, *62*(4), 600-12.
17. Liou, S-C; Chen, S-Y; Lee, H-Y; Bow, J-S. Structural characterization of nano-sized calcium deficient apatite powders. *Biomaterials* **2004**, *25*(2), 189-96.
18. Xu, J.L.; Khor, K.A.; Dong, Z.L.; Gu, Y.W.; Kumar, R.; Cheang, P. Preparation and characterization of nano-sized hydroxyapatite powders produced in a radio frequency (rf) thermal plasma. *Materials Science and Engineering: A* **2004**, *374*(1-2), 101-8.
19. Nie, W.; Peng, C.; Zhou, X.; Chen, L.; Wang, W.; Zhang, Y.; *et al*. Three-dimensional porous scaffold by self-assembly of reduced graphene oxide and nano-hydroxyapatite composites for bone tissue engineering. *Carbon* **2017**, *116*, 325-37.
20. Haidar, Z.S. Biomechanics and Functional Tissue Engineering; IntechOpen: London, United Kingdom, **2021**; pp. 1–268.